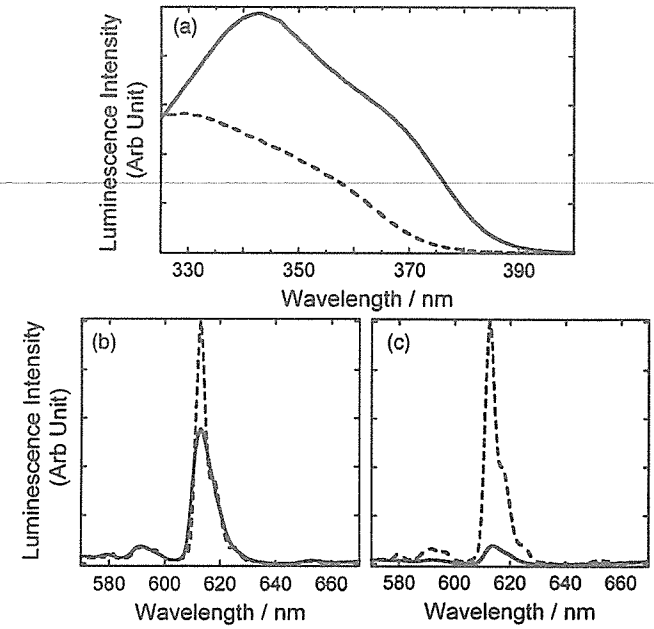

Fig. 3. (a) Excitation spectrum of $Eu(tta)_3phen$ (solid line) and $Eu(bta)_3phen$ (broken line) in benzene (2.00×10^{-7} M). The luminescence intensities were measured at 613 nm. (b, c) Luminescence spectra of the 10.0 wt.% europium-complex-doped polymer particles on a glass substrate. (b) PSt, (c) PMMA. Solid lines and broken lines in (b) and (c) indicate spectra of particles doped with $Eu(tta)_3phen$ and $Eu(bta)_3phen$, respectively. The particles were excited at 360 nm.

From these results shown in Figs. 2 and 3, it is concluded that the best combination of luminescent dopant and matrix polymer is $Eu(bta)_3phen$ and PSt. This may be attributed to the phenyl groups of $Eu(bta)_3phen$ which can blend into the phenyl moiety of PSt polymer.

Following these results, PSt particles doped with trivalent terbium or samarium ion complex coordinated to the same ligands as $Eu(bta)_3phen$ were prepared. Luminescence spectra of the particles are indicated in Fig. 4. Properties of these particles are summarized in Table 1. All particles doped with $Tb(bta)_3phen$ and $Sm(bta)_3phen$ were luminescent as with the case of $Eu(bta)_3phen$ dopant. All luminescence spectra of the lanthanide-complex-doped polymer particles were almost identical with those of dilute solutions of the corresponding lanthanide complexes in benzene. All monodispersity values of the particles were less than 1.05, indicating that they were monodisperse [16]. SEM image of PSt particles, as shown in Fig. 5, revealed their smooth spherical surface with few dimples. This

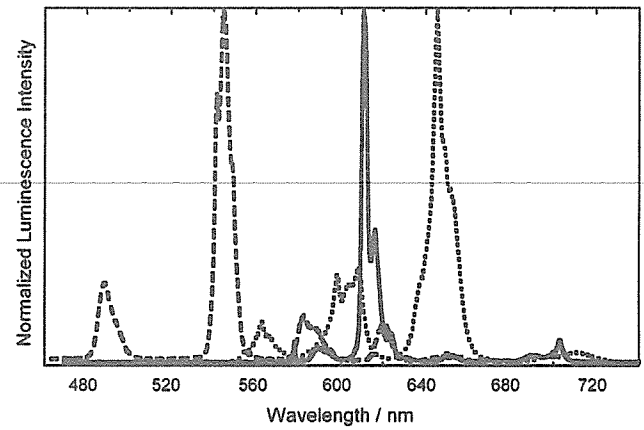

Fig. 4. Luminescence spectra of the 10.0 wt.% lanthanide-complex-doped single PSt particle on a glass substrate, measured by microscopic spectroscopy technique. Solid, broken, and dotted lines indicate spectra of the polymeric particles doped with $Eu(bta)_3phen$, $Tb(bta)_3phen$, and $Sm(bta)_3phen$, respectively. All particles were excited at 330–385 nm UV light from a mercury lamp.

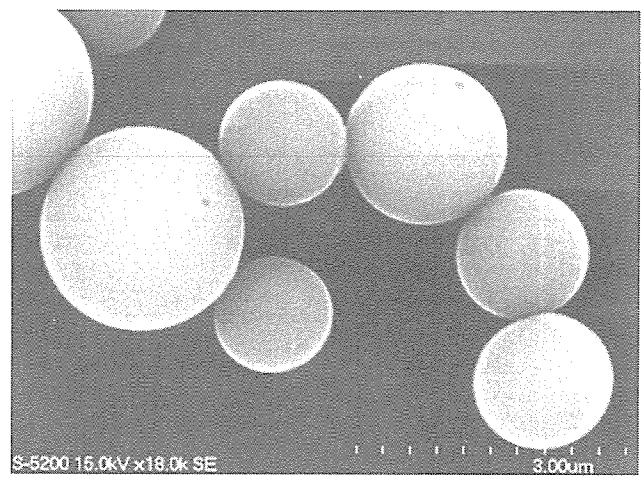

Fig. 5. SEM image of the PSt particles doped with $Sm(bta)_3phen$ at a concentration of 10.0 wt.%.

surface morphology was similar to commercially available PSt particles.

In conclusion, luminescent polymeric particles doped with europium, terbium, and samarium complexes were prepared by the simple self-organized particle precipitation method. Miscibility of the dopant lanthanide lumophore to the matrix polymer

Table 1
Properties of PSt particles doped with the lanthanide complex $M(bta)_3phen$[a]

Dopant lanthanide M	Main emission band		Number-average diameter (μm)	Monodispersity[b]
	Peaktop/nm	FWHM/nm		
Tb	544.8	8.8	2.01	1.04
Eu	610.6	3.3	1.52	1.05
Sm	645.5	7.7	1.62	1.03

[a] Preparation conditions. PSt concentration: 1.00 g/L; lanthanide complex concentration: 10.0 wt.% to the polymer; volume ratio of water to the polymer solution: 1/1.
[b] Calculated from weight-average diameter over number-average diameter.

has an important role in the luminescence properties of the particles. In order to develop new visible and near-infrared luminescent materials, preparation of polymeric particles doped with appropriate lanthanide complexes and organic dyes as lumophore is now in progress.

Acknowledgements

This research was partially supported by Grant-in-Aid for Young Scientists from the Ministry of Education, Culture, Sports, Science and Technology (MEXT) of Japan. The authors appreciate Ms. K. Ito and Ms. S. Yagi for their kind assistance.

References

[1] P. Ball, The Self-made Tapestry: Pattern Formation in Nature, University Press, Oxford, Oxford, 1999.
[2] N. Maruyama, T. Koito, T. Sawadaishi, O. Karthaus, K. Ijiro, N. Nishi, S. Tokura, S. Nishimura, M. Shimomura, Supramol. Sci. 5 (1998) 331–336.
[3] G. Widawski, M. Rawiso, B. François, Nature 369 (1994) 387–389.
[4] M. Srinivasarao, D. Collings, A. Philips, S. Patel, Science 292 (2001) 79–83.
[5] L.V. Govor, I.A. Bashmakov, R. Kiebooms, V. Dyakonov, J. Parishi, Adv. Mater. 13 (2001) 588–591.
[6] M.H. Stenzel, Aust. J. Chem. 55 (2002) 239–243.
[7] B. de Boer, U. Stalmach, H. Nijland, G. Hadziioannou, Adv. Mater. 12 (2000) 1581–1583.
[8] O. Karthaus, N. Maruyama, X. Cieren, M. Shimomura, H. Hasegawa, T. Hashimoto, Langmuir 16 (2000) 6071–6076.
[9] M. Shimomura, Hierarchical structuring of nanostructured 2-dimensional polymer assemblies, in: H. Masuhara, F.C. DeSchryver (Eds.), IUPAC Chemistry for the 21st Century Monograph: Organic Mesoscopic Chemistry, Blackwell Science, Oxford, 1999, pp. 107–126.
[10] H. Yabu, M. Tanaka, K. Ijiro, M. Shimomura, Langmuir 19 (2003) 6297–6300.
[11] H. Yabu, M. Shimomura, Langmuir 21 (2005) 1709–1711.
[12] H. Yabu, M. Takebayashi, M. Tanaka, M. Shimomura, Langmuir 21 (2005) 3235–3237.
[13] H. Yabu, M. Shimomura, Chem. Mater. 17 (2005) 5231–5234.
[14] H. Yabu, T. Higuchi, M. Shimomura, Int. J. Nanosci., in press.
[15] H. Yabu, T. Higuchi, M. Shimomura, Adv. Mater. 17 (2005) 2062–2065.
[16] K. Tamaki, M. Shimomura, Int. J. Nanosci. 1 (2002) 533–537.
[17] K. Tamaki, T. Isoshima, M. Hara, M. Shimomura, Int. J. Nanosci., in press.
[18] S.T. Frey, M.L. Gong, W.D. Horrocks Jr., Inorg. Chem. 33 (1994) 3229–3234.
[19] S.W. Pyo, M.H. Lee, H.S. Lee, J.S. Kim, Y.K. Kim, H.S. Hoe, S.H. Lee, J. Korean Phys. Soc. 35 (1999) S173–S176.
[20] Z.M. Topilova, G.I. Gerasimenko, L.S. Kudryavtseva, M.O. Lozinskii, S.B. Meshkova, Koord. Khim. 16 (1990) 1427–1432.
[21] J.F. Desruex, in: J.-C.G. Bünzli, G.R. Choppin (Eds.), Lanthanide Probes in Life, Chemical and Earth Sciences, Theory and Practice, Elsevier, Amsterdam, 1989, pp. 43–64.

Available online at www.sciencedirect.com
SCIENCE DIRECT
ELSEVIER
Colloids and Surfaces A: Physicochem. Eng. Aspects 284–285 (2006) 505–508
COLLOIDS AND SURFACES A
www.elsevier.com/locate/colsurfa

Simple fabrication of ring-like microwrinkle patterns

Takuya Ohzono [a,*], Masatsugu Shimomura [a,b]

[a] *Dissipative-Hierarchy Structures Laboratory, Spatio-Temporal Function Materials Research Group, Frontier Research System, RIKEN, 2-1 Hirosawa, Wako, Saitama 351-0198, Japan*
[b] *Research Institute for Electronic Science, Hokkaido University, N21W10, Sapporo 001-0021, Japan*

Received 22 July 2005; received in revised form 4 November 2005; accepted 6 November 2005
Available online 15 December 2005

Abstract

Spontaneously formed microwrinkle patterns on a metal-capped elastomer surface are modulated by introducing lithographic structures on the original surface as spatial triggers for directed wrinkle formation. The lithographic patterns are fabricated by utilizing a thin polymer film with hexagonally packed micro pores as a lithographic mask. The wrinkle crests tend to form along the small ridges of the lithographic ring-like structure. We find the compression direction-dependent reversible modulation of the directed wrinkle pattern by compressive strain.

Keywords: Wrinkle; Honeycomb film; Stripe pattern

1. Introduction

As methods for the patterning of a surface at the micrometer, or submicrometer, length scales, various spontaneous processes has been investigated because such procedures are more cost-effective and technologically simpler than those of conventional lithography. For example, phase separation in thin films of block copolymers produces chemically distinct regions [1], dewetting of liquid polymer films produces dot patterns, network structures, and hierarchical assemblies [2,3], self-assembly of transiently passivated water microdroplets on volatile polymer solutions leaves honeycomb-like structures after evaporation of solvents and water [4–10], and mechanical instability of thin films due to in-plane stress induces wrinkles with stripe patterns on elastic/viscoelastic materials after surface hardening by metal depositions or plasma treatments [11–17].

Although most spontaneously formed patterns have characteristic lateral length scales (periodicities of dots, domains and stripes), they largely include spatial fluctuations of the characteristic length scale, random distribution of ordering orientation. Such uncertainties become obstacles to technological applications that require precision. Thus, combinations of lithographic and self-organized methods are required for more efficient use of both methods [18,19] and may give us new unexpected properties.

In this paper, we briefly report that the microwrinkle pattern is modulated by introducing, prior to wrinkle formation, surface lithographic patterns, the lateral length scales of which are close to the average wavelength of the resultant wrinkles. Although the effects of lithographic patterns with much larger length scales than those of wrinkles have been reported [11–14], it remains to be clarified how wrinkle patterns couple to lithographic patterns with approximately the same (or smaller) lateral length scales. The typical microwrinkle pattern, which is formed on a Pt-deposited polydimethylsiloxane (PDMS) elastomer without lithographic patterns under the condition of 2D isotropic residual stress, is a randomly packed mosaic of stripe domains (Fig. 1A), each of which has a specific orientation. The randomness arises from the uncontrollable initial surface imperfections, such as density distribution and roughness, because they locally modulate surface stress states, and subsequently trigger out-of-plane deformation. The introduced lithographic pattern is an ordered pattern of surface heterogeneities that modulate the 2D local stress state regularly. Thus, the resultant wrinkle pattern is directed. We utilize a thin polymer film with hexagonally packed micro pores (Fig. 1B) as the basis for the lithographic pattern.

* Corresponding author.
E-mail address: ohzono@riken.jp (T. Ohzono).

0927-7757/$ – see front matter © 2005 Elsevier B.V. All rights reserved.
doi:10.1016/j.colsurfa.2005.11.016

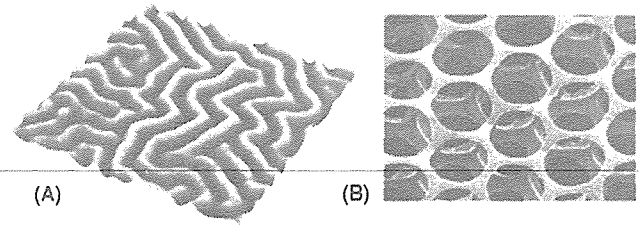

Fig. 1. (A) Atomic force microscopy image (10^2 μm^2, 150 nm for the top to bottom height) of a typical microwrinkle pattern formed on the Pt-sputtered PDMS substrate due to isotropic residual stress. (B) Scanning electron microscopy image (FE-SEM, Hitachi, S-5200) of a thin polymer film with hexagonally packed micro pores utilized as a lithographic mask. The diameter of the hole is ca. 2.8 μm.

2. Experimental

The fabrication process for the modulated microwrinkle structure is schematically shown in Fig. 2, which consists of (1) preparation of the thin film with ordered micro pores; (2) transfer of the film to a bare PDMS surface; (3) oxygen plasma treatment on the PDMS surface using the porous film as a mask; (4) removal of the film; and (5) Pt deposition onto the PDMS surface with a lithographic pattern. Here, the film with ordered micro pores is utilized as a lithographic or etching mask to fabricate an ordered pattern on the PDMS surface, because it is easy to prepare the film and transfer it onto other substrates [6,9,10]. It should be noted that the present method does not include conventional lithographic techniques, which produce the micropatterns directly, such as electron beam lithography. Although we can use such costly techniques for arbitrary patterns, hole-mask lithography serves well to demonstrate the coupling between microwrinkles and small periodic surface imperfections. The details of the fabrication process are described in the results and discussion section.

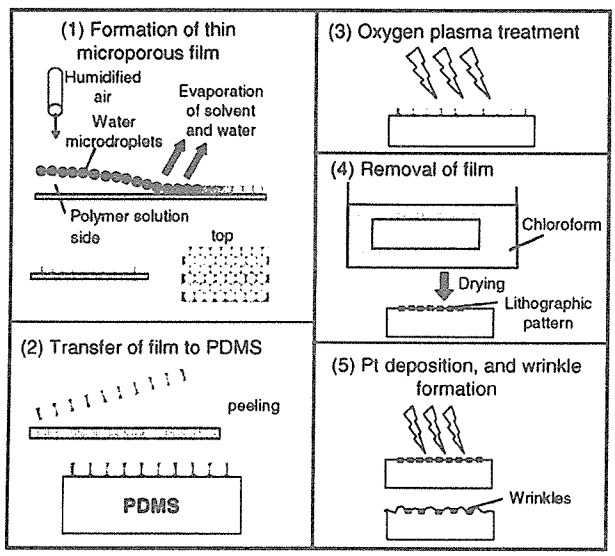

Fig. 2. Schematic of the experimental procedure for fabrication of microwrinkle structures coupled to lithographic patterns of a microporous film.

The responses of modulated wrinkle patterns to uniaxial compressive strain in two different directions with respect to that of the hexagonal lattice were also investigated. The sample was placed in a small vise and subjected to 10% compressive strain. The patterns under strain are observed by the optical microscope (Olympus, BX60).

3. Results and discussion

3.1. Preparation of surfaces with lithographic patterns

The thin films with micropores were prepared on flat glass substrates. We cast 30 mL of benzene solution of the 1:4 mixture of a copolymer, which is composed of dodecylacrylamide and ω-carboxyhexylacrylamide, and the poly(L-lactic acid). Humidified air was blown to the solution surface for water microdroplet condensation. After evaporation of solvent and water the microporous film with pore diameters of approximately 2.8 μm was obtained. For detail of the film preparation refer to other publications [9,10]. The microporous film could be peeled off without substantial deformation. The free-standing film was placed on the PDMS elastomer (Dow Corning, Silpot 184) with a flat surface. The circular areas were exposed to subsequent oxygen plasma treatment.

The oxygen plasma treatment was applied weakly to the PDMS elastomer with the microporous film using a plasma cleaner (South Bay Technology, PC2000) with 24 Pa and 10 W for 10 s. Under this condition, the PDMS surface exposed to oxygen plasma was slightly oxidized and, thus, hardened. After removing the microporous film by rinsing the sample with chloroform, the surface was observed by atomic force microscopy (AFM, Veeco, Explorer TMX2100). The AFM image shows that ring-like ridges with a height of 20–40 nm and width of 200–300 nm along the circular areas were formed, and the relative height of the exposed areas to those protected by the porous film during plasma treatment was 5–8 nm (Fig. 3A). We assume the following scenario for the formation of the topography: (1) the exposed area expanded laterally and vertically during plasma treatment; (2) simultaneously, the area became oxidized

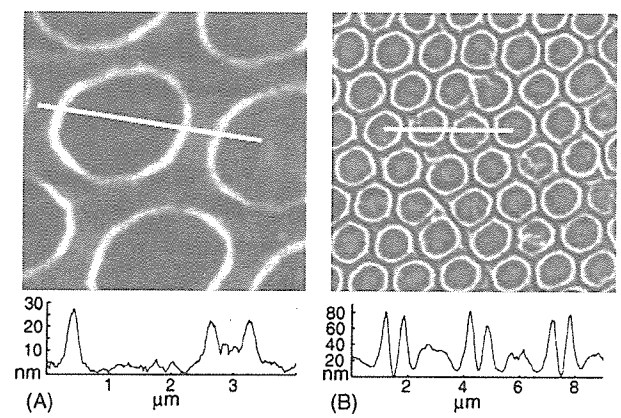

Fig. 3. AFM images observed for each step of the fabrication process. (A) Image (5^2 μm^2) of the lithographic pattern produced by oxygen plasma treatment after removing the microporous film. (B) Image (20^2 μm^2) of the microwrinkle pattern coupled to the lithographic pattern.

and hardened by cross-linking between polymer chains; (3) during/after plasma treatment, the hardened exposed area pushed on the unexposed soft area due to residual stress leading to ridge formation around the boundary of the exposed and unexposed areas, which may account for one of the buckling phenomena; and the vertical expansion of the exposed area remained, leading to the height difference between the exposed and unexposed areas.

3.2. Formation of modulated wrinkles

The deposition of Pt with a thickness of approximately 6 nm was then conducted using an ion sputter (metal coating) apparatus (E-1030, Hitachi) with a current of 5 mA, a pressure of 10 Pa, a distance of 34 mm between samples and the Pt target, and a deposition time of 180 s. During the deposition, the PDMS surface was heated (ca. 100 °C) and expanded due to the collision energy of active metal species. Thus, a hard layer of Pt was formed on the expanded area. As the temperature decreased after deposition, the wrinkle patterns formed [11–14,17].

Fig. 3B shows that the wrinkles were directed by the ring-like lithographic pattern. Basically, wrinkle crests with width of 0.5–0.7 μm appeared along ring-like ridges, and the inner parts of the rings rose slightly. The ring-like ridges triggered the out-of-plane deformation, wrinkling, to relax the residual strain. Although here we only report the case where the wrinkles form simply along the lithographic pattern, there is a variation of coupling between the wrinkles and the lithographic pattern depending on the relative scale of both patterns. Please refer to another study [20] for details.

3.3. Wrinkle patterns under uniaxial compression in two different directions

In a previous study [17], it was reported that wrinkles with a complex stripe pattern were reversibly aligned by compression. Thus, the responses of modulated wrinkle patterns to lateral compression in two different directions with respect to the hexagonal lattice direction were investigated. The sample was subjected to 10% compressive strain. When one of the main axes coincided approximately with the perpendicular direction of strain (commensurate configuration), the straight lines of aligned wrinkles appeared (Fig. 4A). In other cases (incommensurate configuration), a beaded pattern of wrinkles appeared (Fig. 4B). This result indicates that the orientation and structure of wrinkles was restricted by the specific lithographic pattern even under strain. Moreover, the stripe rearrangement processes were reversible at room temperature. In other words, the original pattern was memorized, as expected from previous studies [17,21,22]. Thus, the property of restricted switching of the local surface profile may be utilized for some applications as a stable mobile element.

4. Summary

We briefly reported coupling between spontaneously formed wrinkles and periodic structures due to lithography, where the original ring-like relief (ridge) of the lithographic pattern was simply emphasized by the wrinkles. The present results suggest that the different types of uncertainties, which are intrinsic for patterns formed through spontaneous processes, i.e., fluctuation in the characteristic length scale, randomness in the ordering orientation, and topological defects, can be controlled by introducing the artificial spatial triggers (the pattern of surface heterogeneity).

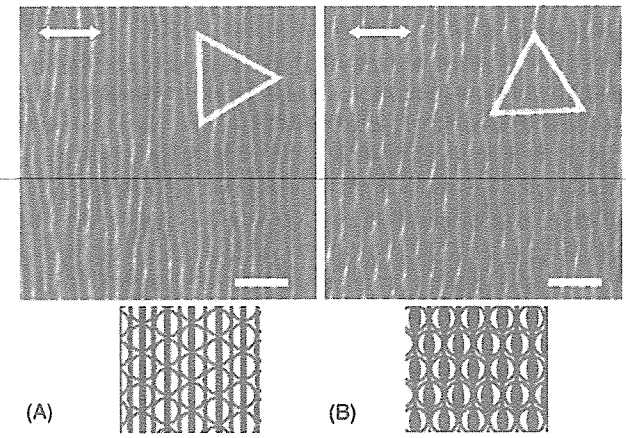

Fig. 4. Optical microscopy images (top) (bar: 5 μm) of the microwrinkle pattern coupled to the lithographic pattern under uniaxial lateral compression of 10% strain in configurations (A) commensurate and (B) incommensurate to the strain direction, and their schematics indicating the relationship between the wrinkle pattern and the lithographic pattern (bottom). The arrows indicate the direction of strain. The triangles express configurations of the three main axes originating from the 2D hexagonal micropore array of the porous film.

The present method to control the surface profile might offer a versatile way to utilize wrinkles, for example, to achieve a desired optical effect, to provide a nano-microarray for spatial storing of small objects with chemical/physical information, or to prepare a controlled substrate for tissue growth. In particular, the combination of the modulated wrinkle patterns and application of external stress, which reversibly controls the wrinkle orientation, may ultimately pave a way of fabricating a mobile surface element for nanomechanical devices, e.g., a gate, router, or mixer for microfluidic systems.

References

[1] G.J. Liu, J.F. Ding, Adv. Mater. 10 (1998) 69.
[2] G. Reiter, Phys. Rev. Lett. 68 (1992) 75.
[3] T. Yamaguchi, N. Suematsu, H. Mahara, in: J.A. Pojman, Q.T.C. Miyata (Eds.), Nonlinear Dynamics in Polymeric Systems, vol. 869, ACS Symp. Ser., 2004, p. 16.
[4] G. Widawski, M. Rawiso, B. Francois, Nature 369 (1994) 387.
[5] S.A. Jenekhe, X.L. Chen, Science 283 (1999) 372.
[6] O. Karthaus, N. Maruyama, X. Cieren, M. Shimomura, H. Hasegawa, T. Hashimoto, Langmuir 16 (2000) 6071.
[7] U. Stalmach, B. de Boer, C. Videlot, P.F. van Hutten, G. Hadziioannou, J. Am. Chem. Soc. 122 (2000) 5464.
[8] T. Yonezawa, S. Onoue, N. Kimizuka, Adv. Mater. 13 (2001) 140.
[9] H. Yabu, M. Tanaka, K. Ijiro, M. Shimomura, Langmuir 19 (2003) 6297.
[10] T. Ohzono, T. Nishikawa, M. Shimomura, J. Mater. Sci. 39 (2004) 2243.
[11] N. Bowden, S. Brittain, A.G. Evans, J.W. Hutchinson, G.M. Whitesides, Nature 393 (1998) 146.

[12] N. Bowden, W.T.S. Huck, K.E. Paul, G.M. Whitesides, Appl. Phys. Lett. 75 (1999) 2557.
[13] D.B.H. Chua, H.T. Ng, S.F.Y. Li, Appl. Phys. Lett. 76 (2000) 721.
[14] W.T.S. Huck, N. Bowden, P. Onck, T. Pardoen, J.W. Hutchinson, G.M. Whitesides, Langmuir 16 (2000) 3497.
[15] J.S. Sharp, R.A.L. Jones, Adv. Mater. 14 (2002) 799.
[16] C.M. Stafford, C. Harrison, K.L. Beers, A. Karim, E.J. Amis, M.R. Vanlandingham, H. Kim, W. Volksen, R.D. Miller, E.E. Simonyi, Nat. Mater. 3 (2004) 545.
[17] T. Ohzono, M. Shimomura, Phys. Rev. B 69 (2004) 132202.
[18] M. Boltau, S. Walheim, J. Mlynek, G. Krausch, U. Steiner, Nature 391 (1998) 877.
[19] H.-L. Zhang, D.G. Bucknall, A. Dupuis, Nano. Lett. 4 (2004) 1513.
[20] T. Ohzono, S.I. Matsushita, M. Shimomura, Soft Matter 1 (2005) 227.
[21] T. Ohzono, M. Shimomura, Jpn. J. Appl. Phys. 44 (2005) 1055.
[22] T. Ohzono, M. Shimomura, Phys. Rev. E 72 (2005) 025203(R).